

Crack initiation direction for in-phase biaxial fatigue loading

V. Chaves¹, C. Madrigal, C. Vallellano, A. Navarro

¹ Departamento de Ingeniería Mecánica, Escuela Superior de Ingenieros, Universidad de Sevilla, Camino de los Descubrimientos s/n, 41092 Sevilla, Spain.

E-mail: chavesrv@us.es

ABSTRACT. *The crack initiation direction in smooth specimens subjected to biaxial fatigue loading is known to depend on material ductility. Thus, in ductile materials cracks initiate mainly in Mode II while in brittle materials they do in Mode I. In this work the ratio between the pure torsion and tension fatigue strength, τ_0/σ_0 is used as an indicator of ductility. Predictions of the crack initiation direction in high cycle fatigue using a microstructural fatigue model that describes the interaction between the crack and the microstructural barriers are shown. The results obtained for both ductile ($\tau_0/\sigma_0 \simeq 0.5$) and fragile ($\tau_0/\sigma_0 \simeq 1$) materials in pure torsion and tension loading are as expected. Besides, the model can predict the initiation direction for different ratios of in-phase biaxial loading and for materials with an intermediate ductility. Predictions are close to the experimental results.*

INTRODUCTION

It is generally accepted that in smooth specimens of ductile materials the initial growth of fatigue cracks seems to be controlled by tangential stresses and thus cracks start growing on the maximum shear stress planes (Mode II - stage I cracks). Once a crack has grown to a certain length, it turns and continues to grow in Mode I (stage II), on the maximum tensile stress plane [1, 2]. This shift in the plane of propagation can be related to the activation of additional slip bands. With fragile materials, however, crack growth seems to be governed by the normal stresses from the start, so the crack initiation and propagation directions coincide with that of the normal to the maximum tensile stress [3]. The ratio between the pure torsion and tension fatigue strengths, τ_0/σ_0 , has been used as an indicator of ductility by several authors [3, 4, 5, 6, 7], which suggest that ductile materials have ratios close to 0.5, whereas fragile materials have values near 1. Most materials exhibit an intermediate degree of ductility and the fatigue strength ratio ranges between 0.5 and 1. See, for example, the extensive experimental work of Gough's group [3] or the experimental data compiled by Fukuda and Nisitani [5]. Thus, there are several experimental examples in the literature showing cracks initiating neither on the maximum principal stress planes nor on planes of maximum shear stress [8, 9].

Calculations of the orientation of the crack initiation plane in high cycle fatigue using

a microstructural fatigue model that describes the interaction between the crack and the microstructural barriers are presented in this work. The results obtained for both ductile ($\tau_0/\sigma_0 \simeq 0.5$) and fragile ($\tau_0/\sigma_0 \simeq 1$) materials in pure torsion and tension loading are as expected. Besides, the model can predict the initiation direction for different ratios of in-phase biaxial loading and for materials with an intermediate ductility. Comparisons with experimental results taken from the literature are also presented.

A MICROSTRUCTURAL MODEL FOR BIAxIAL FATIGUE LIMITS

A microstructural model for fatigue limits under biaxial in-phase loading has been recently presented [10]. It is based on the work of Navarro and de los Rios on monoaxial loads [11] and assumes that plastic slip occurs in linear slip bands running along the grains of the material. Microcracks form in the grains whose size and crystal orientation are most favorable for the formation of persistent slip bands. Each of these cracks expands while its associated plastic zone is halted at a microstructural barrier (usually a grain boundary). The plastic zone remains blocked until the condition to trigger plastic slip in the next grain is fulfilled. The original NR model for monoaxial loading considers a cracks of length $2a$ inside a metal body of infinite size with a mean grain size D under a uniform stress σ . The crack, its plastic zone and the barrier are represented by a continuous distribution of dislocations. The grain boundaries lie at $iD/2$ (with $i = 1, 3, 5, \dots$). It is at those boundaries where the plastic zone will be successively contained. The microstructural barrier is modeled as a small zone of length r_0 , which is the typical size of the interface between grains or the distance to the sources of dislocations that can be triggered in the next grain. The equation describing the equilibrium of the dislocations is a singular integral equation, which is used to calculate the stress σ_3^i needed at the barrier at any time. It can be shown that σ_3^i attains a maximum when the crack tip reaches the barrier. For a freely slipping crack, this maximum is given by:

$$\sigma_3^i = \frac{1}{\cos^{-1} n} \left[\frac{\pi}{2} \sigma \right] \quad (1)$$

where $n = (iD/2)/(iD/2 + r_0)$. The crack will propagate into the next grain if σ_3^i reaches a value high enough for activation of dislocation sources in the neighbouring grain. This critical condition is written as:

$$\frac{\sigma_3^i}{m_i^*} = \tau_c^i \quad (2)$$

where m_i^* is a crystallographic orientation factor projecting σ_3^i onto the plane and slip direction of the dislocation source in the adjacent grain, and τ_c^i is the critical stress needed to activate the source. τ_c^i can be estimated from data obtained in a conventional fatigue test. Alternatively, it can also be derived from a Hall-Petch analysis as shown by Dübér et al. [12]. The fatigue strength of the material is the macroscopic applied stress needed to overcome the barriers in the first grain. Therefore, substituting this value into Eq. 1, and the resulting σ_3^1 value into Eq. 2, the critical stress needed to overcome the first

barrier, $m_1^* \tau_c^1$, can be estimated. The values of the critical stresses needed to surmount the following grain boundaries can be calculated in the similar manner and they can be compared with values measured from the experimental Kitagawa-Takahashi diagram of the material to calculate the successive values of the orientation factor ratios m_i^*/m_1^* , as suggested by de los Rios et. al [13]. If the Kitagawa-Takahashi diagram is not available, an approximate diagram can be obtained by using the equation proposed by El-Haddad using only the experimental values of the threshold K_{th} and the fatigue limit σ_{FL} of the material [14] as done by Chaves and Navarro [15] or the heuristic formula proposed by Vallellano et al. [16]. A model suitable for biaxial in-plane loading uses two distributions

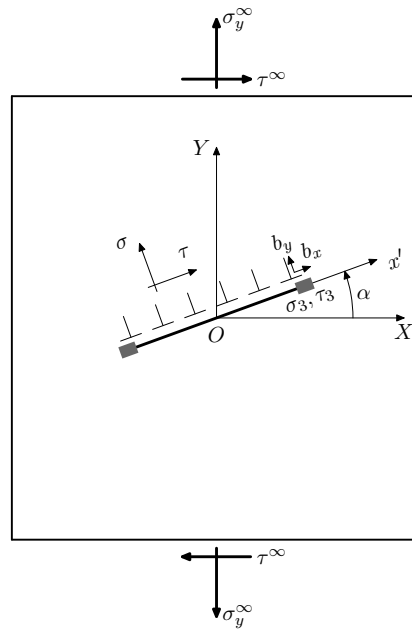


Figure 1. Model for biaxial loading

of dislocations with Burguer's vectors normal (climb) and parallel (glide) to the crack plane, the orientation of which is not known initially. Figure 1 depicts the biaxial model. The body is subjected to both normal σ_y^∞ and tangential τ_y^∞ loads which cause a normal stress σ and a shear stress τ in the crack plane, which lies at an angle α with respect to the X axis. In this case, the barrier is acted upon by both a normal stress σ_3^i and a tangential stress τ_3^i each coming from the corresponding distribution of dislocations. Now the condition for activation of dislocation sources in the neighbouring grain must take into account both components of stress: the source is activated when the sum of the stresses resolved onto the slip plane and slip direction of the source reaches the critical value:

$$\frac{\sigma_3^i}{m_{\sigma_i}^*} + \frac{\tau_3^i}{m_{\tau_i}^*} = \tau_c^i \quad (3)$$

where $m_{\sigma_i}^*$ and $m_{\tau_i}^*$ are now the appropriate crystallographic orientation factors. As in the monoaxial model, solving the equilibrium equations for the two sets of dislocations allows

one to relate σ_3^i and τ_3^i at the barrier, and σ and τ in the crack plane. These relationships are identical to equation 1. Thus, the triggering condition can be formulated as follows for the crack in the first grain, $i = 1$ (see [10] for details):

$$\frac{1}{\cos^{-1} n} \frac{\pi}{2} \left[\frac{\sigma}{m_{\sigma 1}^*} + \frac{\tau}{m_{\tau 1}^*} \right] = \tau_c^1 \quad (4)$$

This equation can be put in a more eloquent form

$$\frac{\sigma}{\sigma_U} + \frac{\tau}{\tau_U} = 1 \quad (5)$$

where $\sigma_U = (\cos^{-1} n)(2/\pi)m_{\sigma 1}^* \tau_c^1$ and $\tau_U = (\cos^{-1} n)(2/\pi)m_{\tau 1}^* \tau_c^1$. Equation 5 represents the *biaxial microscopic activation criterion*. It defines a straight line splitting the $\sigma - \tau$ plane in two regions (see Fig. 2). Please, note carefully that the axes in this figure are the normal (σ) and tangential (τ) stresses at the crack plane. According to the present model, stress combinations above the line will trigger the source of dislocations and cause the crack to propagate beyond the first barrier and eventually lead to failure in a plain specimen. On the other hand, stress combinations below the line will cause cracks to grow only up to the barrier, because plastic slip beyond the barrier can not be triggered. In this situation, the initiated cracks will stop at the barrier and they will remain arrested as long as the applied stresses are not increased.

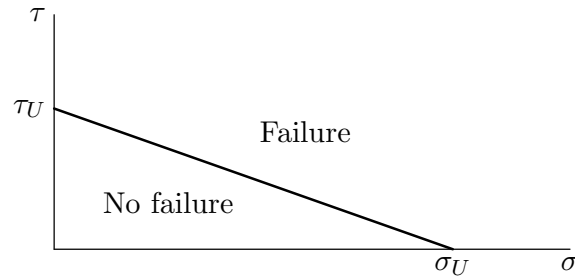


Figure 2. Biaxial microscopic activation criterion (Eq. 5)

The limit microscopic stresses, σ_U and τ_U , and the conventional macroscopic tensile and torsional fatigue strengths can be related examining the corresponding tests via Mohr's circles. Figure 3 shows Mohr's circles for a pure torsional load and a pure tensile load. In a reverse torsion test, the maximum cyclic tangential stress not leading to fatigue failure (or, in other words, the minimum stress needed to cause failure) is obviously the torsional fatigue strength, τ_0 . When the applied stress equals τ_0 , the Mohr's circle will be tangential to the line for the microscopic activation criterion. Likewise, for a cyclic tensile test, the applied tensile stress causing the Mohr's circle to be tangential to the line for the microscopic criterion will be the tensile fatigue strength, σ_0 . Then, the following equation relating σ_U and τ_U to the torsional and tensile fatigue strengths can be derived (see [10], Appendix A, for derivation): if $\bar{\alpha} = \sigma_0/\tau_0$, then

$$\sigma_U = \frac{\sigma_0}{2 - \bar{\alpha}} \quad \tau_U = \frac{\sigma_0}{2\sqrt{\bar{\alpha} - 1}} \quad (6)$$

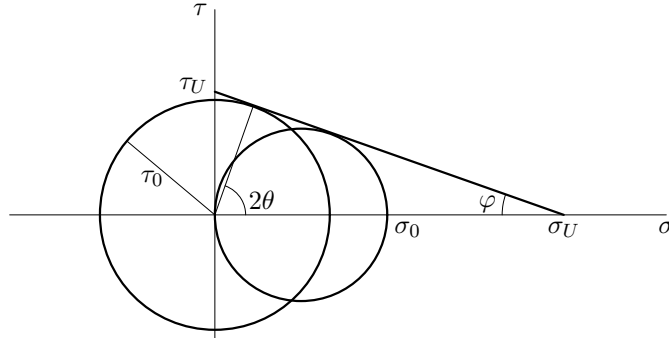


Figure 3. Biaxial microscopic activation criterion and Mohr's circles for pure torsional and pure tensile load

CRACK INITIATION DIRECTIONS

In Fig. 3, the angle 2θ between a line normal to that of the biaxial activation criterion and the horizontal axis σ provides the crack initiation direction according to the model. Such direction corresponds to a plane that forms an angle θ with the direction of the maximum principal stress. Its expression is as follows:

$$\theta = (90^\circ - \arctan(\tau_U/\sigma_U))/2 \quad (7)$$

Perfectly ductile material under pure tension and torsion

For a perfectly ductile material with $\tau_0/\sigma_0 = 0.5$, one has $\bar{\alpha} = 2$ and, based on Eq. 6, the microscopic parameters are $\sigma_U = \infty$ and $\tau_U = \sigma_0/2$. Note that this is a Tresca type material. Figure 4 shows the tensile and torsional Mohr's circles, and the line for the biaxial activation criterion, which is tangential to both circles and it is a horizontal line. Since $2\theta = 90^\circ$, the crack initial direction, θ will be at an angle of 45° with respect to the maximum principal stress direction and it will, therefore, always coincide with the direction of maximum tangential stress. Thus, in a pure axial fatigue test, with the load applied along the Y axis, the crack will start at an angle of $\alpha = 45^\circ$ with respect to the X axis, whereas in a pure torsional fatigue test ($\tau_{YX} = \tau^\infty$ alone in Figure 1), the initiation angle with respect to the X -axis would be $\alpha = 0^\circ$ (or 90°).

Perfectly fragile material under pure tension and torsion

For a perfectly fragile material $\tau_0/\sigma_0 = 1$, thus $\bar{\alpha} = 1$ and the microscopic parameters are $\sigma_U = \sigma_0$ and $\tau_U = \infty$. Figure 5 shows the torsional and tensile Mohr's circles, and the line for the biaxial activation criterion, which is now a vertical line. Therefore, $2\theta = 0^\circ$ and the crack initiation direction will be at an angle of 0° with respect to the maximum principal stress direction, i.e. it will always coincide with the direction of the maximum normal stress. This represents an angle of $\alpha = 0^\circ$ in a pure axial fatigue test

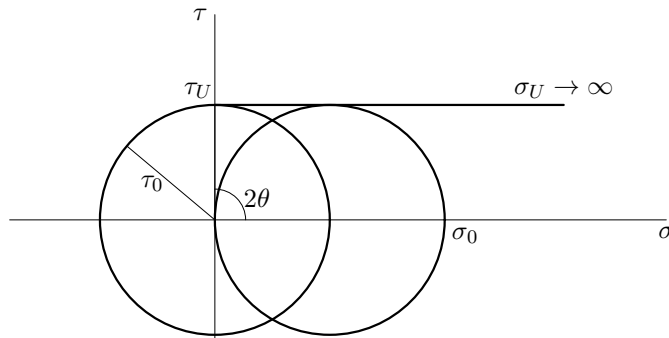


Figure 4. Perfectly ductile material. Microscopic criterion. Mohr's circles for the pure torsion test (left) and pure tension test (right).

and $\alpha = 45^\circ$ in a pure torsional fatigue test (loading directions as in the previous case), again as expected.

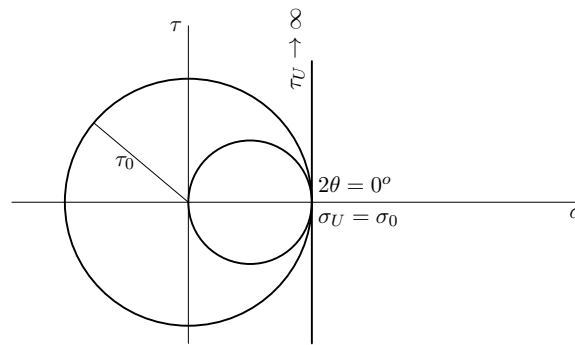


Figure 5. Perfectly fragile material. Microscopic criterion. Mohr's circles for the pure torsion test (outer) and pure tension test (inner).

COMPARISON WITH EXPERIMENTAL RESULTS

The calculations effected with the present model have been compared with some experimental results from the literature. They are summarized in Table 1. The first four columns of this Table show the type of material and test. The next three are related to the crack direction: the fifth column shows the angle α ($^\circ$) observed experimentally, that is the angle that the crack at its origin forms with the X axis of the specimen (again using the notation in figure 1. Please note that the crack direction angles have been estimated from micrographs shown in the referenced articles and therefore they must be taken with some caution. The sixth column displays the prediction of the angle obtained with a classical criterion, that is, the direction of the maximum shear stress for ductile materials and the direction of the maximum principal stress for fragile materials. And the seventh one shows the angles calculated with the present model. The first two rows refer to an experimental work of Murakami and Endo [17]. The material was a low carbon steel, with a value of the ratio $\tau_0/\sigma_0 = 0.59$, very close to the von Mises ratio. The two cracks studied

Table 1. Summary of the experimental results taken from literature and predictions

Material	Ref.	τ_0/σ_0	Test	Crack direction, $\alpha(^{\circ})$		
				Experimental	Classical	Model
0.13%C steel	[17]	0.59	Axial	29	45	39.8
				26	45	39.8
0.45%C steel	[5]	0.59	Torsion	7	0	5.2
0.45%C steel	[9]	0.59	Torsion	5	0	5.2

were both non-propagating, 100 and 50 μm long respectively, observed on the surface of plain specimens subjected to tensile load at the fatigue limit (10^7 cycles). The mean ferrite grain size was 37 μm , so the cracks were presumably longer than one grain. The experimental cracks directions were approximately 29° and 26° respectively, as measured from the Figures 8 and 9 of the article, quite far from either 0° or 45° . Being a ductile material, the prediction with a classical criterion would be 45° . While the prediction with the present model is 39.8° . The third row refers to a work of Fukuda and Nisitani [5]. The material was quite similar to the previous one, but with a smaller mean grain size, just 20 μm . The load was torsion, so the classical criterion would predict the initiation at 0° . The crack shown in the Figure 10 of the article lies at 7° for approximately, 20 μm . The prediction with the model is 5.2° , closer to the experimental direction than the classical criterion. Finally the last experimental work was done by Marquis and Socie [9]. The fatigue strength ratio of the material, τ_0/σ_0 , was not reported by the authors and has just been taken as 0.59, for it is also a low-carbon steel, very similar in composition and tensile properties to the second material. It is a torsion test and the crack approximately starts at 5° respect to the horizontal, which is the direction of the shear stress. The prediction with the model is 5.2° , quite close to the experimental value, although the limitations of the procedure used to estimate the orientation must always be borne in mind.

CONCLUSIONS

- The biaxial microstructural model allows one to predict the crack initiation direction for plane specimens for different ratios of in-phase biaxial loading.
- The model is sensitive to the ductility of the material as defined in terms of the ratio τ_0/σ_0 and predicts that the crack initiation direction for perfectly ductile materials (i.e. materials with $\tau_0/\sigma_0 = 0.5$) will coincide with that of the maximum tangential stress (Mode II), whereas that for perfectly fragile materials ($\tau_0/\sigma_0 = 1$) will be the maximum normal stress direction (Mode I). Both results are as expected according to classical methods.
- The analysis of experimental results has shown that the calculated values of the initiation direction seem to be closer to the experimental ones than the values obtained with the classical criteria by just invoking pure Mode I or Mode II directions.

Acknowledgements

The authors would like to thank the Spanish Ministry of Education for its financial support through grants DPI2008-01100 and DPI2011-27019 and the Junta de Andalucía through grant P07-TEP-03045.

REFERENCES

1. Forsyth PJE. A unified description of micro and macroscopic fatigue crack behaviour. *Int J Fatigue* 1968;5:3-14.
2. Socie DF, Marquis GB., *Multiaxial fatigue*, Chapter 3. SAE International, 2000.
3. Gough HJ, Pollard HV, Clenshaw WJ. Some Experiments on the Resistance of Metals to Fatigue under Combined Stresses. Ministry of Supply, Aeronautical Research Council Reports and Memoranda, London: His Majesty's Stationary Office; 1951 .
4. Sonsino CM. Influence of material's ductility and local deformation mode on multiaxial fatigue response. *Int J Fatigue* 2011;33:930-947.
5. Fukuda T, Nisitani H. The background of fatigue limit ratio of torsional fatigue to rotating bending fatigue in isotropic materials and materials with clear-banded structure. *European Structural Integrity Society* 2003;31:285-302. *Biaxial/Multiaxial Fatigue and Fracture*.
6. Susmel L. *Multiaxial notch fatigue*. Woodhead Publishing; 2009.
7. Carpinteri A, Spagnoli A, Vantadori S. Multiaxial fatigue assessment using a simplified critical plane-based criterion. 2011;33:969-976.
8. Murakami Y. *Metal fatigue: effects of small defects and nonmetallic inclusions*. Elsevier; 2002.
9. Marquis G, Socie D. Long-life torsion fatigue with normal mean stresses. *Fatigue Fract Engng Mater Struct* 2000;23:293-300.
10. Navarro A, Vallellano C, Chaves V, Madrigal C. A microstructural model for biaxial fatigue conditions, *Int J Fatigue* 2011;33:1048-54.
11. Navarro A, de los Rios ER. Fatigue Crack Growth Modelling by Successive Blocking of Dislocations. In: *Proceedings of R. Soc. Lond. A* 1992;437:375-390.
12. Düber O, Künkler B, Krupp U, Christ HJ, Fritzen CP. Experimental characterization and two-dimensional simulation of short crack propagation in an austenitic-ferritic duplex steel. *Int J Fatigue* 2006;28:983-992.
13. de los Rios ER, Navarro A. Consideration of grain orientation and work hardening on short-fatigue-crack modelling. *Phil Mag A* 1990;61:435-439.
14. El Haddad MH, Topper TH, Smith KN. Prediction of non propagating cracks. *Eng Fract Mech* 1979;11:573-84.
15. Chaves V, Navarro A. Application of a microstructural model for predicting notch fatigue limits under Mode I loading. *Int J Fatigue* 2009;31:943-951.
16. Vallellano C, Navarro A, Domínguez J. Fatigue crack growth threshold conditions at notches. Part II: generalization and application to experimental results. *Fatigue Fract Engng Mater Struct* 2000;23:123-28.
17. Murakami Y, Endo T. Effects of small defects on fatigue strength of metals. *Int J Fatigue* 1980;2:23-30.